Maximally random discrete-spin systems with symmetric and asymmetric interactions and maximally degenerate ordering

Maximally random discrete-spin systems with symmetric and asymmetric interactions and maximally degenerate ordering

Bora Atalay[1] and A. Nihat Berker[2,3]

[1]*Faculty of Engineering and Natural Sciences, Sabancı University, Tuzla, Istanbul 34956, Turkey*

[2]*Faculty of Engineering and Natural Sciences, Kadir Has University, Cibali, Istanbul 34083, Turkey*

[3]*Department of Physics, Massachusetts Institute of Technology, Cambridge, Massachusetts 02139, USA*

(Received 20 January 2018; published 2 May 2018)

Discrete-spin systems with maximally random nearest-neighbor interactions that can be symmetric or asymmetric, ferromagnetic or antiferromagnetic, including off-diagonal disorder, are studied, for the number of states $q = 3,4$ in d dimensions. We use renormalization-group theory that is exact for hierarchical lattices and approximate (Migdal-Kadanoff) for hypercubic lattices. For all $d > 1$ and all noninfinite temperatures, the system eventually renormalizes to a random single state, thus signaling $q \times q$ degenerate ordering. Note that this is the maximally degenerate ordering. For high-temperature initial conditions, the system crosses over to this highly degenerate ordering only after spending many renormalization-group iterations near the disordered (infinite-temperature) fixed point. Thus, a temperature range of short-range disorder in the presence of long-range order is identified, as previously seen in underfrustrated Ising spin-glass systems. The entropy is calculated for all temperatures, behaves similarly for ferromagnetic and antiferromagnetic interactions, and shows a derivative maximum at the short-range disordering temperature. With a sharp immediate contrast of infinitesimally higher dimension $1 + \epsilon$, the system is as expected disordered at all temperatures for $d = 1$.

DOI: 10.1103/PhysRevE.97.052102

I. INTRODUCTION: ASYMMETRIC AND SYMMETRIC MAXIMALLY RANDOM SPIN MODELS

Spin models such as Ising, Potts, and ice models show a richness of phase transitions and multicritical phenomena [1,2] that is qualitatively compounded with the addition of frozen (quenched) randomness. Examples are the emerging chaos in spin glasses with competing ferromagnetic and antiferromagnetic (and more recently, without recourse to ferromagnetism versus antiferromagnetism, competing left and right chiral [3]) interactions, the conversion of first-order phase transitions to second-order phase transitions, and the infinite multitude of accumulating phases as devil's staircases. In the current study, frozen randomness is taken to the limit, in $q = 3,4$ state models in arbitrary dimension d, and the results are quite unexpected.

Thus, changes in the critical properties and the phase-transition order are the effects of quenched randomness as well as the appearance of new phenomena such as chaotic rescaling and devil's staircase topologies of phase diagrams. A key microscopic ingredient in these phenomena is the occurrence of frustration, in which all interactions along closed paths in the lattice cannot be simultaneously satisfied. The renormalization-group transformation that we use in this study is equipped to study frustrated systems (and thus has been extensively used in spin-glass systems), as can be seen below from the equivalent hierarchical lattice where closed loops occur corresponding to bond moving following decimation.

The systems that we study are quenched maximally random q-state discrete spin models with nearest-neighbor interactions, with Hamiltonian

$$-\beta\mathcal{H} = -\sum_{\langle ij\rangle} \beta\mathcal{H}_{ij}, \tag{1}$$

where the sum is over nearest-neighbor pairs of sites $\langle ij\rangle$.

The maximal randomness is best expressed in the transfer matrix T_{ij}, e.g., for $q = 3$,

$$\mathbf{T}_{ij} \equiv e^{-\beta\mathcal{H}_{ij}} = \begin{pmatrix} 1 & e^J & 1 \\ 1 & 1 & e^J \\ e^J & 1 & 1 \end{pmatrix}, \begin{pmatrix} 1 & 1 & e^J \\ e^J & 1 & 1 \\ 1 & e^J & 1 \end{pmatrix}, \begin{pmatrix} e^J & 1 & 1 \\ 1 & 1 & e^J \\ 1 & e^J & 1 \end{pmatrix}, \begin{pmatrix} 1 & 1 & e^J \\ 1 & e^J & 1 \\ e^J & 1 & 1 \end{pmatrix}, \begin{pmatrix} 1 & e^J & 1 \\ e^J & 1 & 1 \\ 1 & 1 & e^J \end{pmatrix}, \text{ or } \begin{pmatrix} e^J & 1 & 1 \\ 1 & e^J & 1 \\ 1 & 1 & e^J \end{pmatrix}, \tag{2}$$

where each row and each column has, randomly, a single e^J element, so that there are six such possibilities (for $q = 4$, also studied here, there are 24 such possibilities), and $J > 0$ or $J < 0$, respectively, for ferromagnetic or antiferromagnetic interactions, both of which are treated in this study. The last matrix corresponds to the usual Potts model. In fact, taken by itself as a pure (nonrandom) model, each of these transfer matrices can be mapped to a Potts model by relabeling the spin states in one of the two sublattices, in hypercubic lattices and corresponding hierarchical lattices. Thus, for the ferromagnetic case, for $d > 1$, a low-temperature ferromagnetic phase and a high-temperature disordered phase occur. For the antiferromagnetic case, the low-temperature phase is a critical phase and appears at a higher dimension [4,5].

In Hamiltonian terms, the currently studied quenched random model is

$$-\beta\mathcal{H}_{i,j} = J\delta_{\sigma_i, P(\sigma_j)}, \tag{3}$$

where P is a random permutation of $\{a,b,c\}$. Thus, at a given site i, for a given spin state, say, $s_i = a$, randomly any

one of the spin states $s_j = a,b$, or c of the nearest-neighbor site j is energetically favored (unfavored) for ferromagnetic (antiferromagnetic) interactions. This favor (unfavor) is independently random for each of the nearest neighbors j. Under renormalization-group transformation, all elements of the transfer matrices across the system randomize. Therefore, we have not included in our renormalization-group initial conditions the cases where there is a difference between the less favored two states, to keep the enunciation of the model simple. However, since our renormalization-group trajectories traverse the latter states, we are confident that our results will not be affected by such a subdiscrimination.

The first two possible transfer matrices on the right side of Eq. (1) represent asymmetric interaction, in the sense that the nearest-neighbor states $(s_i,s_j) = (a,b)$ and (b,a) have different energies, where $s_i = a$, b, or c are the $q = 3$ possible states of a given site i. Asymmetric interactions occur in neural network systems [6] and are largely unexplored in statistical mechanics. On the other hand, the last four possible transfer matrices on the right side of Eq. (1) exemplify symmetric interaction, the nearest-neighbor states $(s_i,s_j) = (a,b)$ and (b,a) having the same energies. As also explained below, even when starting with only symmetric interactions (the last four matrices), asymmetric interactions are generated under renormalization-group transformations [as can be seen, e.g., by multiplying the third and fifth matrices in Eq. (2), corresponding to a renormalization-group decimation] and the same ordering results are obtained. Thus, asymmetric interactions are generated by off-diagonal (symmetric) disorder. The generalization of the above model to arbitrary q is obvious.

II. RENORMALIZATION-GROUP TRANSFORMATION

The renormalization-group method is readily implemented to the transfer matrix form of the interactions. The quenched randomness aspect of the problem is included by randomly creating 500 transfer matrices from the six possibilities of Eq. (1) and perpetuating these random 500 transfer matrices throughout the renormalization-group steps given below. Note that we start with a single initial value of J, which is proportional to the inverse temperature. Quenched randomness comes from the positioning within the matrix. Under renormalization-group transformation, each matrix element evolves quantitatively quenched randomly.

The renormalization-group transformation begins with the "bond-moving" step in which b^{d-1} transfer matrices, each randomly chosen from the 500, have their corresponding matrix elements multiplied. This operation is repeated 500 times, thus generating 500 new transfer matrices. The final, "decimation" step of the renormalization-group transformation is the matrix multiplication of b transfer matrices, again each randomly chosen from the 500. This operation is also repeated 500 times, again generating 500 renormalized transfer matrices. The length rescaling factor is taken as $b = 2$ in our calculation. At each transfer-matrix calculation above, each element of the resulting transfer matrix is divided by the largest element, resulting in a matrix with the largest element being unity. This does not affect the physics, since it corresponds to subtracting a constant from the Hamiltonian. These subtractive constants (the natural logarithm of the dividing element) are scale-accumulated, as explained below, for the calculation of entropy.

The above transformation is the approximate Migdal-Kadanoff [7,8] renormalization-group transformation for hypercubic lattices and, simultaneously, the exact renormalization-group transformation of a hierarchical lattice [9–11]. This procedure has been explained in detail in previous work [3]. For most recent exact calculations on hierarchical lattices, see Refs. [12–19], including finance [18] and DNA-binding [19] problems.

III. ASYMPTOTICALLY DOMINANT ALL-TEMPERATURE FREEZING IN $d > 1$ WITH HIGH-TEMPERATURE SHORT-RANGE DISORDERING

Figure 1 shows the renormalization-group trajectories for the system with $q = 3$ states in $d = 3$ dimensions, starting at three different temperatures $T = J^{-1}$, where J refers to the renormalization-group-trajectory initial conditions shown in Eqs. (2) and (3). Shown are the second (J_2) and third (J_3) largest values of the energies (dimensionless, being temperature-divided) that appear exponentiated in the transfer matrix elements,

$$J_{ij} = \ln(T_{ij}), \tag{4}$$

averaged over the quenched random distribution, where T_{ij} are the elements of the $q \times q$ transfer matrix $\mathbf{T}_{ij}$. The matrix average of the eight nonleading energies $< J_{2-9} >$, averaged over the quenched random distribution, is also shown. The leading energy is $J_1 = 0$ by subtractive overall constant, as explained above. As seen in this figure, starting at low temperature $T = 2$, the system renormalizes to a state in which the leading energy is totally dominant, all other energies renormalizing to $-\infty$. The matrix position of the single asymptotically dominant element occurs randomly among the $q \times q$ possibilities, including off-diagonal and therefore necessarily asymmetric, but is the same across the quenched random distribution. The number of possible dominant transfer-matrix elements gives the degeneracy of the ordered phase, so that with $q \times q$, maximal degeneracy is achieved. A diagonal element of the transfer matrix being dominant means that one state, e.g., $s_i = c$, dominates at the strong coupling fixed point and characterizes the ordered phase. This does have the usual permutational symmetry of the Potts model, being physically equivalent to all diagonal elements dominating, but with nondiagonal elements zero so that only one spin state dominates the entire physical system. The equivalence is not complete only in the fact that the latter picture allows different domains in the system, whereas the former does not. A nondiagonal element $T_{km} = 1$ being dominant maintains itself by having T_{im},T_{kj}, where $i \neq k, j \neq m$, being small, decreasing under renormalization group, but nonzero. The corresponding spin state is highly degenerate, as can be seen from the renormalization-group solution, where each spin has a degeneracy of 2 (still less than the disordered number of q), seen at decimation transformations, and the system is randomly populated by two spin states corresponding to the indices k and m of the dominant T_{km}.

Moreover, starting at high temperatures, as seen, e.g., in the left and center panels of Fig. 1, the system spends many renormalization-group iterations near the infinite-temperature

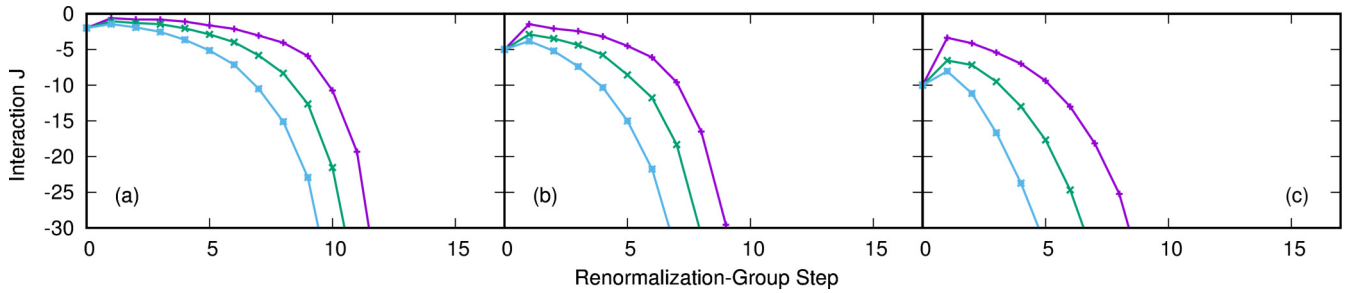

FIG. 1. Renormalization-group trajectories for the system with $q = 3$ states in $d = 3$ dimensions, starting at three different temperatures $T = J^{-1}$ from Eqs. (2) and (3), namely starting with (a) $J = 0.02$, (b) $J = 0.20$, (c) $J = 0.50$. Shown are the second (J_2) and third (J_3) largest values and the matrix average of the eight nonleading energies $< J_{2-9} >$ of the transfer matrix [Eq. (4)], averaged over the quenched random distribution. The leading energy is $J_1 = 0$ by subtractive choice. The different starting values can be seen on the left axis of each panel (corresponding to renormalization-group step 0). Starting at any nonzero temperature, the system renormalizes to a state in which the leading energy is totally dominant, all other energies renormalizing to $-\infty$. The matrix position of the single asymptotically dominant element occurs randomly among the $q \times q$ possibilities including off-diagonal and therefore necessarily asymmetric, but is the same across the quenched random distribution. However, starting at high temperatures, as seen, e.g., in the left and center panels, the system spends many renormalization-group iterations near the infinite-temperature fixed point (where all energies are zero), before crossing over to the ordered fixed point. Since the energies at a specific step of a renormalization-group trajectory directly show the effective couplings across the length scale that is reached at that renormalization-group step, this behavior indicates islands of short-range disorder at the short length scales that correspond to the initial steps of a renormalization-group trajectory. These islands of short-range disorder nested in long-range order have been explicitly calculated and shown in spin-glass systems in Ref. [20]. These islands of short-range disorder occur in the presence of long-range order, since the trajectories eventually flow to the strong-coupling fixed point. As temperature is increased (changing the renormalization-group initial condition), these short-range disordered regions order, giving rise to the smooth specific heat peak but no phase transition singularity, as there is no additional fixed-point structure underlying this short-range ordering.

fixed point (where all energies are zero), before crossing over to the ordered fixed point. This signifies short-range disorder, in the presence of long-range order, as also reflected in the specific heat peaks caused by short-range disordering as discussed below. A similar smeared transition to short-range disorder in the presence of long-range order has previously been seen in underfrustrated Ising spin-glass systems [22].

We have repeated our calculations for noninteger spatial dimensions approaching $d = 1$ from above, by keeping the bond-moving number $b^{d-1} = 2$ and increasing the decimation number b. The behavior described above obtains for all $d \gtrsim 1$, albeit with an increasing high-temperature range of short-range disorder, and higher number of renormalization-group steps to strong coupling, as $d = 1$ is approached. At $d = 1$, the infinite-temperature fixed point is the sole attractor, and the system is disordered at all temperatures.

IV. FREE ENERGY, ENTROPY, AND SPECIFIC HEAT

The renormalization-group solution gives the complete equilibrium thermodynamics for the systems studied. The dimensionless free energy per bond $f = F/kN$ is obtained by summing the additive constants generated at each renormalization-group step,

$$f = \frac{1}{N} \ln \sum_{\{s_i\}} e^{-\beta \mathcal{H}} = \sum_{n=1} \frac{G^{(n)}}{b^{dn}}, \tag{5}$$

where N is the number of bonds in the initial unrenormalized system, the first sum is over all states of the system, the second sum is over all renormalization-group steps n, $G^{(n)}$ is the additive constant generated at the nth renormalization-group transformation averaged over the quenched random distribution, and the sum quickly converges numerically.

From the dimensionless free energy per bond f, the entropy per bond S/kN is calculated as

$$\frac{S}{kN} = f - J \frac{\partial f}{\partial J}, \tag{6}$$

and the specific heat C/kN is calculated as

$$\frac{C}{kN} = T \frac{\partial (S/kN)}{\partial T} = -J \frac{\partial (S/kN)}{\partial J}. \tag{7}$$

Figures 2–4 give the calculated free energies f, entropies S/kN, and specific heats C/kN per bond as functions of temperature $T = J^{-1}$, for $q = 3,4$ states in $d = 3,4$ dimensions. The expected $T = \infty$ values of $f = \ln q/(b^d - 1)$ and

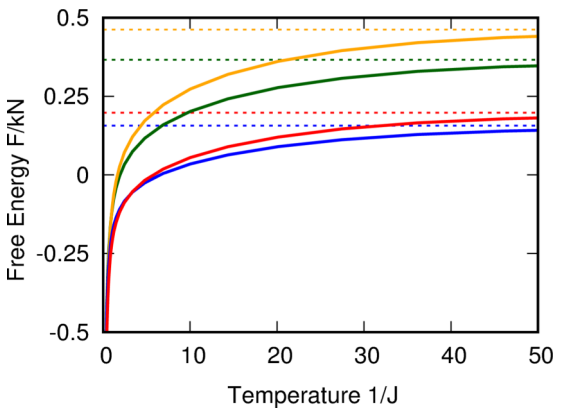

FIG. 2. Calculated free energy per bond as a function of temperature $T = J^{-1}$. The curves are, from top to bottom, for ($q = 4,d = 2$), ($q = 3,d = 2$), ($q = 4,d = 3$), and ($q = 3,d = 3$). The expected $T = \infty$ values of $f = F/kN = \ln q/(b^d - 1)$ are given by the dashed lines and match the calculations.

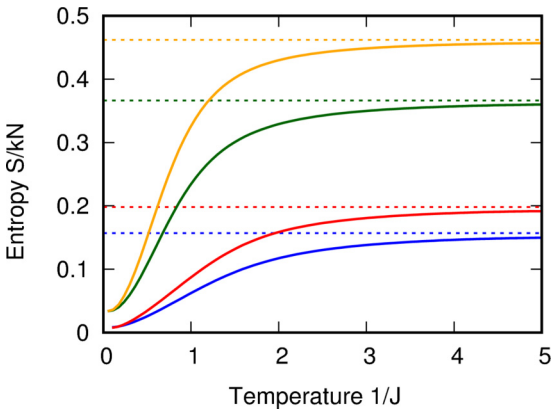

FIG. 3. Calculated entropy per bond as a function of temperature $T = J^{-1}$, for $q = 3,4$ states in $d = 3,4$ dimensions. The curves are, from top to bottom, for $(q = 4,d = 2)$, $(q = 3,d = 2)$, $(q = 4,d = 3)$, and $(q = 3,d = 3)$. The expected $T = \infty$ values of $S/kN = \ln q/(b^d - 1)$ are given by the dashed lines and match the calculations.

$S/kN = \ln q/(b^d - 1)$ are given by the dashed lines and match the calculations.

As explained in Fig. 1, the specific heat maximum occurs at the temperature of the short-range disordering. In this figure, starting at high temperatures, as seen, e.g., in the left and center panels, the system spends many renormalization-group iterations near the infinite-temperature fixed point (where all energies are zero), before crossing over to the ordered fixed point. Since the energies at a specific step of a renormalization-group trajectory directly show the effective couplings across the length scale that is reached at that renormalization-group step, this behavior indicates islands of short-range disorder at the short length scales that correspond to the initial steps of a renormalization-group trajectory. These islands of short-range disorder nested in long-range order have been explicitly calculated and shown in spin-glass systems in Ref. [20]. These islands of short-range disorder occur in the presence of long-range order, since the trajectories eventually flow to

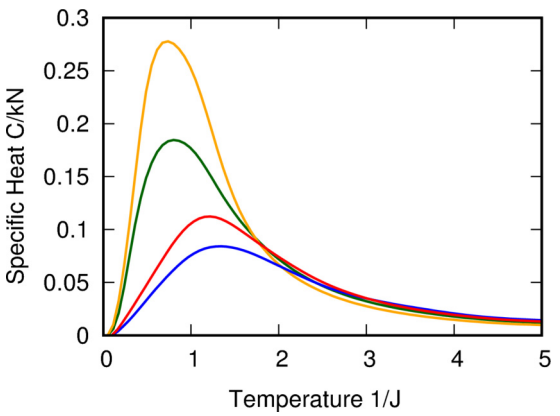

FIG. 4. Calculated specific heat as a function of temperature $T = J^{-1}$, for $q = 3,4$ states in $d = 3,4$ dimensions. The curves are, from top to bottom, for $(q = 4,d = 2)$, $(q = 3,d = 2)$, $(q = 4,d = 3)$, $(q = 3,d = 3)$. A specific heat maximum occurs at short-range disordering.

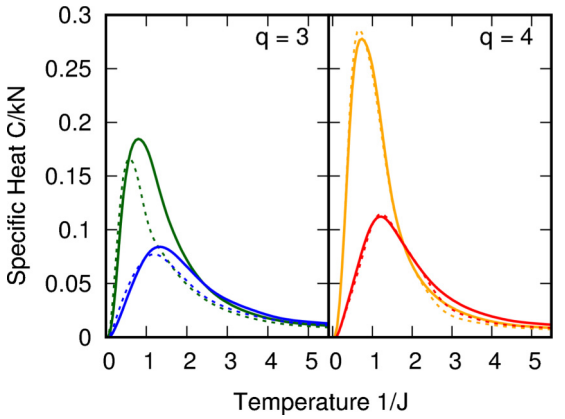

FIG. 5. Calculated specific heat as a function of temperature $T = |J|^{-1}$ for ferromagnetic $(J > 0)$, full curves, and antiferromagnetic $(J < 0)$, dashed curves, systems, for $q = 3,4$ states in $d = 3,4$ dimensions. The curves are, from top to bottom in each panel, for $d = 2$ and $d = 3$. The quantitatively same short-range disordering behavior is seen for both ferromagnetic and antiferromagnetic systems.

the strong-coupling fixed point. As temperature is increased (changing the renormalization-group initial condition), these short-range disordered regions order, giving rise to the smooth specific heat peak, but no phase transition singularity, as there is no additional fixed-point structure underlying this short-range ordering. Specific heat maxima away from phase transitions, due to short-range ordering, have been calculated in a variety of systems [21,22].

V. ANTIFERROMAGNETIC MAXIMALLY RANDOM SYSTEMS

We have repeated our calculations for antiferromagnetic $(J < 0)$ systems and obtained quantitatively similar behavior. Figure 5 shows the calculated specific heats as a function of temperature $T = |J|^{-1}$ for ferromagnetic $(J > 0)$ and antiferromagnetic $(J < 0)$ systems, for $q = 3,4$ states in $d = 3,4$ dimensions. The full-temperature range $(T < \infty)$ maximally degenerate long-range ordering and a quantitatively same short-range disordering at high temperature are seen for both ferromagnetic and antiferromagnetic systems.

VI. CONCLUSION

We have studied maximally random discrete-spin systems with symmetric and asymmetric interactions and have found, quite surprisingly, (1) quenched random long-range order at all noninfinite temperatures for $d > 1$ and (2) short-range disordering at high temperatures, via a smeared transition and a specific-heat peak, while sustaining long-range order. The latter behavior has also been seen in underfrustrated Ising spin-glass systems [22].

ACKNOWLEDGMENTS

Support by the Academy of Sciences of Turkey (TÜBA) is gratefully acknowledged. We thank Tolga Çağlar for most useful discussions.

[1] B. Nienhuis, A. N. Berker, E. K. Riedel, and M. Schick, Phys. Rev. Let. **43**, 737 (1979).
[2] G. Delfino and E. Tartaglia, Phys. Rev. E **96**, 042137 (2017).
[3] T. Çağlar and A. N. Berker, Phys. Rev. E **96**, 032103 (2017).
[4] A. N. Berker and L. P. Kadanoff, J. Phys. A **13**, L259 (1980).
[5] A. N. Berker and L. P. Kadanoff, J. Phys. A **13**, 3786 (1980).
[6] Edited by E. Domany, J. L. van Hemmen, and K. Schulten, editors, *Models of Neural Networks* (Springer-Verlag, Berlin, 1991).
[7] A. A. Migdal, Zh. Eksp. Teor. Fiz. **69**, 1457 (1975) [Sov. Phys. JETP **42**, 743 (1976)].
[8] L. P. Kadanoff, Ann. Phys. (NY) **100**, 359 (1976).
[9] A. N. Berker and S. Ostlund, J. Phys. C **12**, 4961 (1979).
[10] R. B. Griffiths and M. Kaufman, Phys. Rev. B **26**, 5022 (1982).
[11] M. Kaufman and R. B. Griffiths, Phys. Rev. B **30**, 244 (1984).
[12] N. Masuda, M. A. Porter, and R. Lambiotte, Phys. Rep. **716-717**, 1 (2017).
[13] S. Li and S. Boettcher, Phys. Rev. A **95**, 032301 (2017).
[14] P. Bleher, M. Lyubich, and R. Roeder, J. Math. Pures Appl. **107**, 491 (2017).
[15] H. Li and Z. Zhang, Theor. Comp. Sci. **675**, 64 (2017).
[16] J. Peng and E. Agliari, Chaos **27**, 083108 (2017).
[17] T. Nogawa, arXiv:1710.04014 [cond-mat.stat-mech] (2017).
[18] Š. J. Širca and M. Omladic, ARS Math. Contemp. **13**, 63 (2017).
[19] J. Maji, F. Seno, A. Trovato, and S. M. Bhattacharjee, J. Stat. Mech.: Theory Exp. (2017) 073203.
[20] D. Yeşilleten and A. N. Berker, Phys. Rev. Lett. **78**, 1564 (1997).
[21] A. N. Berker and D. R. Nelson, Phys. Rev. B **19**, 2488 (1979).
[22] E. Ilker and A. N. Berker, Phys. Rev. E **89**, 042139 (2014).